ICASSP 2022 - 2022 IEEE International Conference on Acoustics, Speech and Signal Processing (ICASSP) | 978-1-6654-0540-9/22/$31.00 ©2022 IEEE | DOI: 10.1109/ICASSP43922.2022.9746201

r-LOCAL UNLABELED SENSING: IMPROVED ALGORITHM AND APPLICATIONS

Ahmed Ali Abbasi[†] *Abiy Tasissa*[⋆] *Shuchin Aeron*[†]

[†] Department of ECE, Tufts University, Medford, MA 02155
[⋆] Department of Mathematics, Tufts University, Medford, MA 02155

ABSTRACT

The unlabeled sensing problem is to solve a noisy linear system of equations under unknown permutation of the measurements. We study a particular case of the problem where the permutations are restricted to be r-local, i.e. the permutation matrix is block diagonal with $r \times r$ blocks. Assuming a Gaussian measurement matrix, we argue that the r-local permutation model is more challenging compared to a recent sparse permutation model. We propose a proximal alternating minimization algorithm for the general unlabeled sensing problem that provably converges to a first order stationary point. Applied to the r-local model, we show that the resulting algorithm is efficient. We validate the algorithm on synthetic and real datasets. We also formulate the 1-d unassigned distance geometry problem as an unlabeled sensing problem with a structured measurement matrix.

Index Terms— Unlabeled sensing, unassigned distance geometry problem, proximal alternating minimization.

1. INTRODUCTION

The standard least squares problem is to recover signal $\mathbf{X}^* \in \mathbb{R}^{d\times m}$ given measurements $\mathbf{Y} \in \mathbb{R}^{n\times m}$ and the measurement matrix $\mathbf{B}$. The signal matrix $\mathbf{X}^*$ is estimated by solving the least squares minimization problem $\min_{\mathbf{X}} \|\mathbf{Y}-\mathbf{B}\mathbf{X}\|_F^2$. This formulation assumes that there is one to one correspondence between measurements (the rows of $\mathbf{Y}$) and the measurement vectors (the rows of $\mathbf{B}$), i.e., we know which measurement corresponds to what measurement vector. However, in many problems of applied interest such as header free communication for mobile wireless networks [1], sampling in the presence of clock jitter [2], linear regression without correspondence [3] and point cloud registration [4], this mapping is not explicitly given. This motivates the study of the unlabeled sensing problem with the prototypical form given by

$$\mathbf{Y} = \mathbf{P}^*\mathbf{B}\mathbf{X}^* + \mathbf{W}, \tag{1}$$

where $\mathbf{P} \in \mathbb{R}^{n\times n}$ denotes the unknown permutation matrix and $\mathbf{W} \in \mathbb{R}^{n\times m}$ denotes an additive Gaussian noise with $\mathbf{W}_{ij} = \mathcal{N}(0, \sigma^2)$. The problem is to estimate $\mathbf{X}^*$ and $\mathbf{P}^*$ given the measurement matrix $\mathbf{B}$ and measurements $\mathbf{Y}$.

Related work: The unlabeled sensing problem was first considered with a Gaussian measurement matrix $\mathbf{B}$ in the single-view setup, where $m = 1$, in [5]. There, the authors showed that $n = 2d$ noiseless measurements are necessary and sufficient for recovery of $\mathbf{x}^*$. The same result was subsequently proven in [6] using an algebraic argument. For the case of Gaussian $\mathbf{B}$, the work in [7] showed that with SNR $\triangleq \|\mathbf{X}^*\|_F^2/m\sigma^2$, SNR $= \Omega(n^2)$ is necessary for recovering $\mathbf{P}^*$ exactly. For the multi-view setup, where $m > 1$, the result in [8] shows that the necessary SNR for recovery decreases as m increases, with necessary SNR $= O(1)$ for $m = \Omega(\log n)$.

Several algorithms have been proposed for the single view unlabeled sensing problem [1, 7, 9]. Algorithms for the multi-view problem setup have been proposed in works [8, 10, 11, 12, 13]. As computing the maximum likelihood estimate of $\mathbf{P}^*$ may be NP-hard [11], the works in [8, 10, 12] impose a k-sparse structure on $\mathbf{P}^*$ (see Figure 1a) where $n-k$ elements of the permutation are on the diagonal. In [13], the authors introduced the r-local model (see section 2) along with an algorithm that is based on graph matching. A permutation matrix $\mathbf{P}^*$ of size $n \times n$ is r-local if it is composed of n/r blocks. Formally, $\mathbf{P}^* = \text{diag}\left(\mathbf{P}_1^*, \cdots, \mathbf{P}_{n/r}^*\right)$, where $\mathbf{P}_i^* \in \Pi_r$ denotes an $r \times r$ permutation matrix (see Figure 1b).

Applications: In this paper, we consider two applications of the r-local unlabeled sensing model. The first application is the unassigned distance geometry problem (uDGP) [14] (see section 3). The second application is image unscrambling [15] (see section 5). Another application of the r-local permutation model is linear regression with blocking [16].

Contributions: (a) We compare the r-local model with the k-sparse model and argue that the r-local problem is more challenging under the most widely studied case of Gaussian measurement matrix. (b) We formulate the 1-d unassigned distance geometry problem (uDGP) [14] as an unlabeled sensing problem with a structured measurement matrix. (c) We propose a proximal alternating minimization algorithm for the r-local unlabeled sensing problem. Simulation results show that the proposed algorithm outperforms the algorithms in [8, 11, 13]. We also compare the proposed algorithm with [12] to show that algorithms for the k-spare model are not applicable to the r-local model.

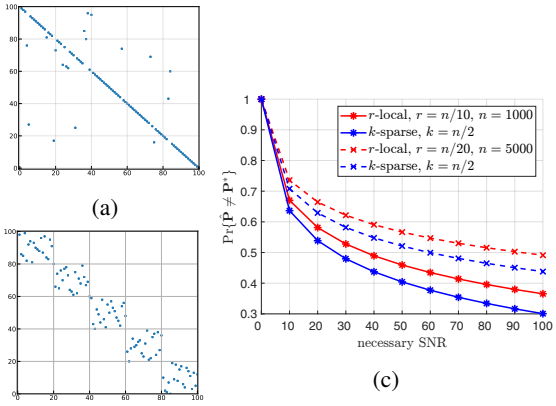

(a)

(b)

(c)

Fig. 1: (a). A sparse (or partially shuffled) permutation considered in [8, 10, 12, 17]. (b). The r-local permutation structure considered in this paper, with $r = 20$. (c). Figure plots the lower bound on the event $\Pr\{\widehat{\mathbf{P}} \neq \mathbf{P}^*\}$ against SNR for the two models (see equation (2)).

2. r-LOCAL MODEL VS k-SPARSE MODEL

A permutation matrix $\mathbf{P}$ is k-sparse if $n-k$ of its elements are on the diagonal, i.e., $\langle \mathbf{I}, \mathbf{P} \rangle = n - k$. Figures 1a and 1b show a k-sparse and an r-local permutation matrix, respectively. We compare the two models by the difficulty of recovering $\mathbf{P}^*$ under each model when the matrix $\mathbf{B}$ is assumed to be random Gaussian. Under this assumption, for any estimator $\widehat{\mathbf{P}}$, the probability of error $\Pr\{\widehat{\mathbf{P}} \neq \mathbf{P}^*\}$ is lower bounded by the result in [8]

$$\Pr\{\widehat{\mathbf{P}} \neq \mathbf{P}^*\} \geq 1 - \frac{1 + \frac{nm}{2} \log_2(1 + \text{SNR})}{H(\mathbf{P}^*)}, \qquad (2)$$

where $\mathbf{P}^*$ is a random variable and $H(\mathbf{P}^*)$ denotes the entropy of $\mathbf{P}^*$. For uniformly distributed $\mathbf{P}^*$, the entropy is $H(\mathbf{P}^*) = \log_2 a$, where a is the number of possible permutations. Without any assumption on the permutation structure, the entropy of $\mathbf{P}^* \in \mathbb{R}^{n \times n}$ is $H(\mathbf{P}^*) = \log_2(n!)$. The entropy for r-local permutations is $H_r(\mathbf{P}^*) = \log_2 r!^{n/r}$. The entropy for k-sparse permutations is $H_k(\mathbf{P}^*) = \log_2(n!/(n-k)!)$. Performance guarantees for proposed algorithms are given for $k = n/8$ in [8] and $k = n/4$ in [12]. All simulation results for permutation recovery in [10, 17] are for $k \leq n/2$. Figure 1c shows that, for the same SNR, the lower bound in (2) is higher for the r-local model, $r = \{n/10, n/20\}$, than for the k-sparse model, with $k = n/2$. This suggests that permutation recovery under the r-local model is challenging in the large n regime.

3. 1-D UNASSIGNED DISTANCE GEOMETRY AS AN UNLABELED SENSING PROBLEM

The one-dimensional unassigned distance geometry problem (1-d uDGP) (see Figure 2) is to recover point coordinates

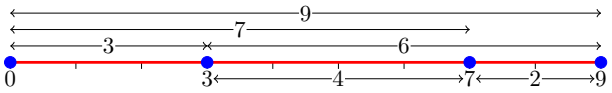

Fig. 2: The 1-d unassigned distance geometry problem (uDGP) is to recover the point coordinates $(0, 3, 7, 9)$ from their unlabeled pairwise distances $\{3, 2, 4, 6, 7, 9\}$. uDGP can be formulated as an unlabeled sensing problem with a deterministic measurement matrix $\mathbf{B}_u$, see equation (3).

from their unlabeled pairwise distances [14, 18, 19]. The distances are unlabeled as the pair (i, j) corresponding to the distance $|x_i - x_j|$ is not known. Let $\overline{\mathbf{x}} \in \mathbb{R}^d = [\overline{x}_1, \cdots, \overline{x}_d]^\intercal$ be the vector of unknown coordinates. Without loss of generality, we assume that the unknown point coordinates are sorted in decreasing order. It follows that each pairwise distance $\overline{x}_i - \overline{x}_j$ is a linear measurement of $\overline{\mathbf{x}}$. As the distances are translation invariant, we can also assume that the left most point is at the origin. The distance vector $\mathbf{y} \in \mathbb{R}^{d(d-1)/2}$ is the matrix-vector product $\mathbf{y} = \mathbf{B}_u \mathbf{x}^*$ where $\mathbf{x}^* \in \mathbb{R}^{d-1}$. It can be verified that $\mathbf{B}_u$ has the following form.

$$\mathbf{B}_u = [\mathbf{I}_{(d-1)\times(d-1)}; \mathbf{B}_2; \cdots; \mathbf{B}_{d-1}],$$
$$[\mathbf{B}_i \in \mathbb{R}^{(d-i)\times(d-1)}]_{pq} = \begin{cases} 1 & \text{if } q = i-1 \\ -1 & \text{if } q = p+i-1 \\ 0 & \text{otherwise,} \end{cases} \qquad (3)$$

where $[\mathbf{A}_1; \mathbf{A}_2]$ denotes vertical concatenation of the matrices $\mathbf{A}_1, \mathbf{A}_2$. The unlabeled sensing formulation for the example in Figure 2, with $d = 4$ points, is given below

$$\underbrace{\begin{pmatrix} 3 \\ 2 \\ 4 \\ 6 \\ 7 \\ 9 \end{pmatrix}}_{\mathbf{y}} = \underbrace{\begin{pmatrix} 0&0&1&0&0&0 \\ 0&0&0&1&0&0 \\ 0&0&0&0&0&1 \\ 0&0&0&0&1&0 \\ 0&1&0&0&0&0 \\ 1&0&0&0&0&0 \end{pmatrix}}_{\mathbf{P}^*} \underbrace{\begin{pmatrix} 1&0&0 \\ 0&1&0 \\ 0&0&1 \\ 1&-1&0 \\ 1&0&-1 \\ 0&1&-1 \end{pmatrix}}_{\mathbf{B}_u} \underbrace{\begin{pmatrix} 9 \\ 7 \\ 3 \end{pmatrix}}_{\mathbf{x}^*}.$$

Why r-local model for uDGP? Imposing an r-local structure on $\mathbf{P}^*$ has a practical interpretation for the uDGP problem. The problem where, in addition to the distances $|x_i - x_j|$, one of the two corresponding indices (i, j) is known, is modelled by an r-local $\mathbf{P}^* = \text{blkdiag}(d-1, \cdots, 2)$. The r-local structure also models the problem where distance assignments are known up to a cluster of points. For example, for two clusters, each distance is known to be between a pair of points in cluster 1 or cluster 2 (intra-cluster) or a point in cluster 1 and a point in cluster 2 (inter-cluster) but the pair of points corresponding to each distance is still unknown.

4. PROPOSED APPROACH AND ALGORITHM

In this section, we present a new algorithm for the r-local unlabeled sensing problem. To motivate our proposed algorithm, we note that for i.i.d Gaussian noise $\mathbf{W}$ in (1), the maximum likelihood estimate of $\mathbf{P}^*$ is given by

$$\underset{\mathbf{X}, \mathbf{P} \in \Pi_n}{\arg\min} F(\mathbf{X}, \mathbf{P}) = \|\mathbf{Y} - \mathbf{P}\mathbf{B}\mathbf{X}\|_F^2, \qquad (4)$$

where Π_n denotes the set of permutations of order n. The optimization problem in (4) is non-convex since the set of permutations is discrete. A natural optimization scheme for the problem in (4) is the alternating minimization algorithm which alternates between updating the signal matrix $\mathbf{X}$ and the permutation $\mathbf{P}$. The works in [10, 11, 12, 17] propose one step estimators for $\mathbf{P}^*, \mathbf{X}^*$. We consider complete alternating minimization for (4) yielding the following updates

$$\mathbf{P}^{(t)} = \underset{\mathbf{P}\in\Pi_n}{\operatorname{argmin}} \langle -\mathbf{Y}\mathbf{X}^{(t)\intercal}\mathbf{B}^\intercal, \mathbf{P}\rangle, \tag{5}$$

$$\mathbf{X}^{(t+1)} = \underset{\mathbf{X}}{\operatorname{argmin}} \; F(\mathbf{X}, \mathbf{P}^{(t)}) = (\mathbf{P}^{(t)}\mathbf{B})^\dagger \mathbf{Y}. \tag{6}$$

The iterates $(\mathbf{P}^{(t)}, \mathbf{X}^{(t+1)})$ above are monotonically decreasing $F(\mathbf{P}^{(t+1)}, \mathbf{X}^{(t+1)}) \leq F(\mathbf{P}^{(t)}, \mathbf{X}^{(t+1)})$. However, this is not sufficient to establish convergence of the iterates. Specifically, we can not claim that $\lim_{t\to\infty}\{(\mathbf{P}^{(t)}, \mathbf{X}^{(t)})\}$ exists. We propose to use proximal alternating minimization (PAM) [20] instead which, as we show in section 4.1, converges to a first order stationary point of the objective in (4). PAM adds a regularization term that encourages the new iterate to be close to the current iterate. Formally, for the objective in (4), the PAM updates are given by

$$\mathbf{P}^{(t)} = \underset{\mathbf{P}\in\Pi_n}{\operatorname{argmin}} \; F(\mathbf{X}^{(t)}, \mathbf{P}) + \lambda^{(t)}\|\mathbf{P} - \mathbf{P}^{(t-1)}\|_F^2, \tag{7}$$

$$\mathbf{X}^{(t+1)} = \underset{\mathbf{X}}{\operatorname{argmin}} \; F(\mathbf{X}, \mathbf{P}^{(t)}) + \lambda^{(t)}\|\mathbf{X} - \mathbf{X}^{(t)}\|_F^2, \tag{8}$$

where $\lambda^{(t)} > 0$. Our algorithm follows from the updates in (7) and (8). Similar to (5) and (6), the updates are a linear program and a regularized least squares problem, respectively. Assuming an r-local structure on $\mathbf{P}^*$, the update in (7) is equivalent to the simpler update of n/r blocks of size r. A summary of our algorithm is given in Algorithm 1.

Algorithmic details: We use the *collapsed* initialization, as also done in [13], to initialize $\widehat{\mathbf{Y}}^{(0)} = \mathbf{B}\widehat{\mathbf{X}}^{(0)}$. The initialization estimates $\widehat{\mathbf{X}}$ from n/r measurements given by summing r consecutive rows in $\mathbf{B}$ and $\mathbf{Y}$. The convergence criteria is based on the relative change in the objective $(F^{(t-1)} - F^{(t)})/F^{(t-1)}$. The total cost of updating all the local permutations by linear programs is $O(nr^2)$. In line 8, $\dagger$ denotes the Moore-Penrose pseudo-inverse. The regularized least squares problem can be solved in $O(2nd^2 - \frac{2}{3}d^3)$,

4.1. Convergence analysis

Proposition 1. *The sequence of iterates* $\{(\mathbf{X}^{(t)}, \mathbf{P}^{(t)})\}$ *generated by* (7)*,* (8) *converges to a first order stationary point of the objective in* (4)*.*

Proof. The result follows from Theorem 9 in [20]. To use Theorem 9, we need to verify that the Kurdyka-Lojasiewicz (KL) inequality holds for the objective $F(\mathbf{X}, \mathbf{P}) = \|\mathbf{Y} - \mathbf{P}\mathbf{B}\mathbf{X}\|_F^2 + \mathbf{I}_C(\mathbf{P})$ where $\mathbf{I}_C(\mathbf{P})$ is the indicator function of the set of permutations. First, note that the set of permutations of order n is semi-algebraic because each of the $n!$ permutations can be specified via n^2 linear equality constraints.

Algorithm 1 Proximal Alt-Min for r-local unlabeled sensing

Input: $\mathbf{B}, \mathbf{Y}, \widehat{\mathbf{Y}}^{(0)}, \widehat{\mathbf{X}}^{(0)}, r, \lambda, \epsilon$
Output: $\widehat{\mathbf{P}}$

1: $t \leftarrow 0$
2: $\widehat{\mathbf{P}}_k^{(t)} \leftarrow \mathbf{1}_{r\times r}/r$
3: **while** relative change $> \epsilon$ **do**
4: **for** $k \in 1 \cdots n/r$ **do**
5: $\widehat{\mathbf{P}}_k = \underset{\mathbf{P}_k\in\Pi_r}{\operatorname{argmin}} \; -\langle \mathbf{Y}\widehat{\mathbf{Y}}^{(t)} + \lambda\widehat{\mathbf{P}}_k^{(t)}, \mathbf{P}_k\rangle$
6: **end for**
7: $\widehat{\mathbf{P}}^{(t+1)} \leftarrow \operatorname{diag}(\widehat{\mathbf{P}}_1, \cdots, \widehat{\mathbf{P}}_{n/r})$
8: $\widehat{\mathbf{X}}^{(t+1)} \leftarrow \left[\frac{\mathbf{B}_{n\times d}}{\sqrt{\lambda}\mathbf{I}_{d\times d}}\right]^\dagger \left[\frac{\widehat{\mathbf{P}}^{(t+1)\intercal}\mathbf{Y}}{\sqrt{\lambda}\widehat{\mathbf{X}}^{(t)}}\right]$
9: $\widehat{\mathbf{Y}}^{(t+1)} \leftarrow \mathbf{B}\widehat{\mathbf{X}}^{(t+1)}$
10: $t \leftarrow t + 1$
11: **end while**

The indicator function of a semi-algebraic function is a semi-algebraic function [20]. The first term in the objective is polynomial, and therefore real-analytic. The sum of a real-analytic function and a semi-algebraic function is sub-analytic, and sub-analytic functions satisfy the KL inequality [21].

5. EXPERIMENTS

For all experiments using Algorithm 1, we set the tolerance $\epsilon = 0.01$. The proximal regularization is set to $\lambda^{(1)} = 100$ and scaled as $\lambda^{(t+1)} = \lambda^{(t)}/10$. MATLAB code for the experiments is available at the first author's github account: github.com/aabbas02/Proximal-Alt-Min-for-ULS-UDGP.

5.1. Synthetic simulations

Data generation: The entries of the signal matrix $\mathbf{X}^*$, the sensing matrix $\mathbf{B}$, and the noise $\mathbf{W}$ are sampled i.i.d. from the normal distribution. The matrix $\mathbf{W}$ is subsequently scaled by σ to set a specific SNR. The permutation $\mathbf{P}^*$ is picked uniformly at random from the set of r-local permutations. All results are averages of 75 Monte Carlo (MC) runs.

Baselines: We compare our algorithm to four algorithms proposed in [8, 11, 12, 13]. First is a biconvex relaxation of (4) proposed in [8] and solved via the alternating direction method of multipliers (ADMM) algorithm. Second is the Levsort algorithm in [11]. For $m = d$ views and $\sigma^2 = 0$, the Levsort algorithm provably recovers $\mathbf{P}^*$ exactly. The third algorithm in [12] approximates $\widehat{\mathbf{X}} \simeq \mathbf{B}^\intercal\mathbf{Y}$ in (5) and estimates $\widehat{\mathbf{P}} = \operatorname{argmin}_{\mathbf{P}\in\Pi}\langle \mathbf{Y}\mathbf{Y}^\intercal\mathbf{B}\mathbf{B}^\intercal, \mathbf{P}\rangle$. The approximation is justified when matrix $\mathbf{B}$ is Gaussian i.i.d. and the rows of $\mathbf{B}$ are partially shuffled. In order to ensure a fair comparison with the algorithms in [8, 11, 12], we specify an additional constraint to constrain the permutation solutions to be r-local. For each MC run, the ADMM penalty parameter ρ for [8] was tuned in the range 10^{-3} to 10^5 and the best results were retained. We also compare to the algorithm in [13] that solves a quadratic assignment problem to estimate $\mathbf{P}^*$. We refer to the

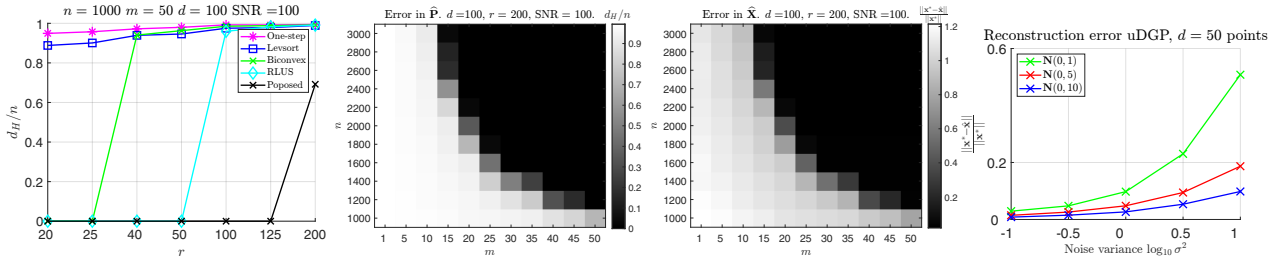

(a) (b) (c) (d)

Fig. 3: **Synthetic simulations** for $\mathbf{Y} = \mathbf{P}^*\mathbf{B}_{n\times d}\mathbf{X}^*_{d\times m} + \mathbf{W}$. (a). Figure plots the fractional Hamming distortion d_H/n against block size r. The Hamming distortion is the number of mismatches in estimate $\widehat{\mathbf{P}}$ of $\mathbf{P}^*$ and is defined as $d_H = \Sigma_i \mathbb{1}(\widehat{\mathbf{P}}(i) \neq \mathbf{P}^*(i))$, where $\mathbf{P}(i)$ denotes the column index of the 1 entry in the i^{th} row of the permutation matrix $\mathbf{P}$. (b,c). Figures plot d_H/n and the relative error $\|\widehat{\mathbf{X}} - \mathbf{X}^*\|/\|\mathbf{X}^*\|$, respectively, against (m, n) for fixed (d, r). (d). **uDGP**. Figure plots the relative error in the estimated point coordinates against increasing noise variance σ^2. The $d = 50$ points are sampled i.i.d. from the normal distribution with variances $\{1, 5, 10\}$, and the permutation $\mathbf{P}^*$ is r-local with blocks of sizes $(d-1, \cdots, 2)$.

(a) PSNR $= 27.04$ dB (b) PSNR $= 11.79$ dB

Fig. 4: (a). Left. Unscrambled image $\mathbf{y} \in \mathbb{R}^n$, $n = 48 \times 42$ from the YALE B dataset. Middle. Scrambled input image $\mathbf{P}^*\mathbf{y}$ via an r-local permutation, $r = 96$. Right. Reconstructed image $\hat{\mathbf{y}} = \widehat{\mathbf{P}}^\intercal\mathbf{P}^*\mathbf{y}$. (b). Left: Unscrambled image $\mathbf{y} \in \mathbb{R}^n$, $n = 28 \times 28$ from the MNIST dataset. Middle: Scrambled input image via an r-local permutation, $r = 28$. Right: Reconstructed image. The peak signal to noise ratio PSNR is defined in terms of the mean square reconstruction error $e = \frac{1}{n}\|\mathbf{y} - \hat{\mathbf{y}}\|_2^2$ as PSNR $= 10\log_{10}(\frac{1}{e^2})$.

algorithms in [8, 11, 12, 13] as 'Biconvex', 'Levsort, 'One-step', and 'RLUS', respectively.

Results: In Figure 3a, we compare our proposed algorithm to the baselines. One-step [12] fails to recover $\mathbf{P}^*$ for even small values of r, underscoring that algorithms to recover sparse permutations cannot be adapted to the r-local model. The Levsort algorithm [11] also fails to recover $\mathbf{P}^*$. The Biconvex algorithm [8] only recovers $\mathbf{P}^*$ for $r = 20$. RLUS [13] gives comparable recovery of $\mathbf{P}^*$ when $r \leq 50$, but is outperformed by the proposed algorithm at higher values of r. In Figures 3b and 3c, we set $(d, r) = (100, 200)$ and vary (n, m). The errors in $\widehat{\mathbf{X}}, \widehat{\mathbf{P}}$ decrease as n increases. This is because the initialization to the algorithm (see section 4) improves with increasing n. The estimates also improve with increasing m. This observation agrees with the discussion in section 1 and the result in (2).

5.2. Scrambled image restoration

We consider a variation of the problem in [15]. Therein, given scrambled images $\mathbf{P}^*\mathbf{y}$ and unscrambled training data $\mathbf{y}$, a neural network is trained to unscramble $\mathbf{P}^*\mathbf{y}$. For our experiment, the images are drawn from the YALE B dataset [22] and the MNIST dataset [23]. For each class in the MNIST (YALE B) dataset, the matrix $\mathbf{B} \in \mathbb{R}^{n\times d}$ contains the $d = 5$ (10) principal components of the unscrambled data. A class in the MNIST (YALE B) dataset comprises all images corresponding to a single digit (particular face). The problem is to recover the unknown permutation $\mathbf{P}^*$ given the scrambled image $\mathbf{P}^*\mathbf{y}$ and the matrix $\mathbf{B}$. The setup is summarized in Figure 4. We compare our algorithm to RLUS [13] and the results are given in Table 1. The results show that the proposed algorithm outperforms RLUS [13].

	Proposed	RLUS [13]
MNIST	$\mathbf{12.31} \pm 2.57$	12.03 ± 2.47
YALE	$\mathbf{28.30} \pm 2.87$	26.43 ± 2.95

Table 1: Scrambled image restoration problem. For each dataset, the PSNR values (dB) are averaged over 10 classes.

5.3. 1-d uDGP

We consider the 1-dimensional uDGP problem (Section 3) where the distances are corrupted with i.i.d. Gaussian noise of variance σ^2. The results in Figure 3d show that the relative error in the recovered points is low even for high noise variance. The results are noteworthy because the general 1-d uDGP problem with noisy distances is NP-hard [24].

6. CONCLUSION

We propose a proximal alternating minimization algorithm for the unlabeled sensing problem and apply it to the setting where the unknown permutation is r-local. The resulting algorithm is efficient and theoretically converges to a first order stationary point. Experiments on synthetic and real data show that the algorithm outperforms competing baselines. We formulate the 1-d unassigned distance geometry problem (uDGP) as an unlabeled sensing problem with a structured measurement matrix. Future work will explore information-theoretic inachieviability results for the r-local permutation model and uDGP.

7. REFERENCES

[1] L. Peng, X. Song, MC Tsakiris, H. Choi, L. Kneip, and Y. Shi, "Algebraically-initialized expectation maximization for header-free communication," in *IEEE Int. Conf. on Acous., Speech and Signal Process. (ICASSP)*. IEEE, 2019, pp. 5182–5186.

[2] A. Balakrishnan, "On the problem of time jitter in sampling," *IRE Trans. on Inf. Theory*, vol. 8, no. 3, pp. 226–236, 1962.

[3] Zhidong Bai and Tailen Hsing, "The broken sample problem," *Probability theory and related fields*, vol. 131, no. 4, pp. 528–552, 2005.

[4] Manuel Marques, Marko Stošić, and João Costeira, "Subspace matching: Unique solution to point matching with geometric constraints," in *2009 IEEE 12th Int. Conf. on Computer Vision*, 2009, pp. 1288–1294.

[5] Jayakrishnan Unnikrishnan, Saeid Haghighatshoar, and Martin Vetterli, "Unlabeled sensing with random linear measurements," *IEEE Trans. Inf. Theory*, vol. 64, no. 5, pp. 3237–3253, 2018.

[6] I. Dokmanić, "Permutations unlabeled beyond sampling unknown," *IEEE Signal Processing Letters*, vol. 26, no. 6, pp. 823–827, 2019.

[7] A. Pananjady, M. J. Wainwright, and T. A. Courtade, "Linear regression with shuffled data: Statistical and computational limits of permutation recovery," *IEEE Trans. Inf. Theory*, vol. 64, no. 5, pp. 3286–3300, 2018.

[8] H. Zhang, M. Slawski, and P. Li, "Permutation recovery from multiple measurement vectors in unlabeled sensing," in *2019 IEEE Int. Symposium on Inf. Theory (ISIT)*, 2019, pp. 1857–1861.

[9] L. Peng and M.C. Tsakiris, "Linear regression without correspondences via concave minimization," *IEEE Signal Proces. Letters*, vol. 27, pp. 1580–1584, 2020.

[10] M. Slawski, E. Ben-David, and P. Li, "Two-stage approach to multivariate linear regression with sparsely mismatched data.," *J. Mach. Learn. Res.*, vol. 21, no. 204, pp. 1–42, 2020.

[11] A. Pananjady, M. J. Wainwright, and T. A. Courtade, "Denoising linear models with permuted data," in *2017 IEEE Int. Symposium on Inf. Theory (ISIT)*, 2017, pp. 446–450.

[12] Hang Zhang and Ping Li, "Optimal estimator for unlabeled linear regression," in *Proceedings of the 37th Int. Conf. on Machine Learning (ICML)*, 2020.

[13] Ahmed Ali Abbasi, Abiy Tasissa, and Shuchin Aeron, "R-local unlabeled sensing: A novel graph matching approach for multiview unlabeled sensing under local permutations," *IEEE Open Journal of Signal Process.*, vol. 2, pp. 309–317, 2021.

[14] Shuai Huang and Ivan Dokmanic, "Reconstructing point sets from distance distributions," *IEEE Trans. Signal Process.*, vol. 69, pp. 1811–1827, 2021.

[15] Gonzalo Mena, David Belanger, Scott Linderman, and Jasper Snoek, "Learning latent permutations with gumbel-sinkhorn networks," 2018.

[16] P. Lahiri and M. D Larsen, "Regression analysis with linked data," *Jrnl of the American statistical association*, vol. 100, no. 469, pp. 222–230, 2005.

[17] M. Slawski, M. Rahmani, and Ping Li, "A sparse representation-based approach to linear regression with partially shuffled labels," in *Uncertainty in Artificial Intelligence*. PMLR, 2020, pp. 38–48.

[18] P. Duxbury, C. Lavor, L. Liberti, and L. de Salles-Neto, "Unassigned distance geometry and molecular conformation problems," *Journal of Global Optimization*, pp. 1–10, 2021.

[19] Tamara Dakic, *On the turnpike problem*, Simon Fraser University BC, Canada, 2000.

[20] H. Attouch, J. Bolte, P. Redont, and A. Soubeyran, "Proximal alternating minimization and projection methods for nonconvex problems: An approach based on the kurdyka-Łojasiewicz inequality," *Mathematics of Operations Research*, vol. 35, no. 2, pp. 438–457, 2010.

[21] Yangyang Xu and Wotao Yin, "A block coordinate descent method for regularized multiconvex optimization with applications to nonnegative tensor factorization and completion," *SIAM Journal on imaging sciences*, vol. 6, no. 3, pp. 1758–1789, 2013.

[22] A.S. Georghiades, P.N. Belhumeur, and D.J. Kriegman, "From few to many: illumination cone models for face recognition under variable lighting and pose," *IEEE Trans. on Pattern Analysis and Machine Intelligence*, vol. 23, no. 6, pp. 643–660, 2001.

[23] Li Deng, "The mnist database of handwritten digit images for machine learning research," *IEEE Signal Processing Magazine*, vol. 29, no. 6, pp. 141–142, 2012.

[24] Mark Cieliebak and Stephan Eidenbenz, "Measurement errors make the partial digest problem np-hard," in *Latin American Symposium on Theoretical Informatics*. Springer, 2004, pp. 379–390.